Electronic Supplementary Material (ESI) for Physical Chemistry Chemical Physics.

Supplementary Note 1: Validation of Reaxff potential

An Qi compared the elastic constants of boron carbide with the DFT results and experimental values when fitting the Reaxff potential function. The elastic constants calculated by the Reaxff potential show good agreement with experimental and QM values.[1] To further verify the reliability of the Reaxff potential, the follow parameters are calculated by molecular dynamics simulation using the Rexaff potential and compared with DFT results and published experimental results.

(1) Lattice parameters of the hexagonal boron carbide crystal.

(2) Cohesive energy of the hexagonal boron carbide crystal.

Lattice parameters

Our simulations focus on the most stable (B11Cp)-CBC variant in boron carbide crystals. We replicated the hexagonal boron carbide unit cell as an 8×14×8 supercell along the x, y, and z axes and use the ReaxFF potential function[1] to relax the supercell. We carried out isothermal-isobaric (NPT) ensemble to relax the model at 300 K using the Nosé-Hoover thermostat and barostat (50-fs damping constant for temperature and 2000-fs damping constant for pressure). The integration time step was set to 0.25 fs run for 50,000 steps. The calculated lattice parameters of the hexagonal boron carbide crystal are shown in Table S1.

The simulation results show that the lattice parameters of boron carbide calculated by the Reaxff potential are very close to the DFT results. The results obtained by Reaxff potential and DFT are slightly deviated from the experimental values, especially in the angle parameters. This is because the C atoms in polar boron carbide occupy the polar sites in the icosahedron, resulting in a small monoclinic distortion.

Table S1 Lattice parameters of boron carbide from the current work compared to literature data.

Lattice parameters	a (Å)	b (Å)	c (Å)	α (º)	β (º)	γ (º)
Ivashchenko et al.[2] (DFT)	5.548	5.548	11.865	91.74	88.26	119.89
Xianming Li et al.[3] (DFT)	5.532	5.532	11.907	92.034	87.966	119.887
Morosin et al.[4] (Experiment)	5.589	5.589	12.054	90	90	120
Reaxff relaxed	5.521	5.521	11.932	93.175	86.623	119.533

Cohesive energy

Using the Reaxff potential, we calculated the cohesive energy of the polar boron carbide, and the calculation results are shown in the Table S2. The result calculated by the Reaxff potential function is closer to the DFT-LDA result and both are slightly higher than the DFT-GGA result. Overall, the Reaxff potential still maintains good consistency with DFT in terms of calculating cohesive energy.

Table S2 Cohesive energy of boron carbide from the current work compared to literature data.

Cohesive energy (eV/atom)	Reaxff	DFT-GGA[5]	DFT-LDA[6]
Boron carbide	-7.021	-6.500	-7.259

In summary, through the calculation of the crystal constants and cohesive energy of boron carbide crystals, we found that the calculated results of the Reaxff potential function are very close to the DFT results and experimental results. It indicates that it is reliable to use the Reaxff potential function fitted by An Qi in LAMMPS to calculate the polar boron carbide. In particular, the Reaxff potential function has been successfully applied to the calculation of high-pressure and impact resistance of boron carbide ceramics.[3, 7-12]

Supplementary Note 2: Effect of loading strain rate

We applied different shear rates of 0.05 ps^{-1}, 0.1 ps^{-1}, 0.15 ps^{-1}, and 0.2 ps^{-1} to the boron carbide model to calculate the effect of shear strain rate on the stress-strain relationship. The calculated stress-strain relationship of boron carbide with different shear strain rates is shown

in Fig. S1.

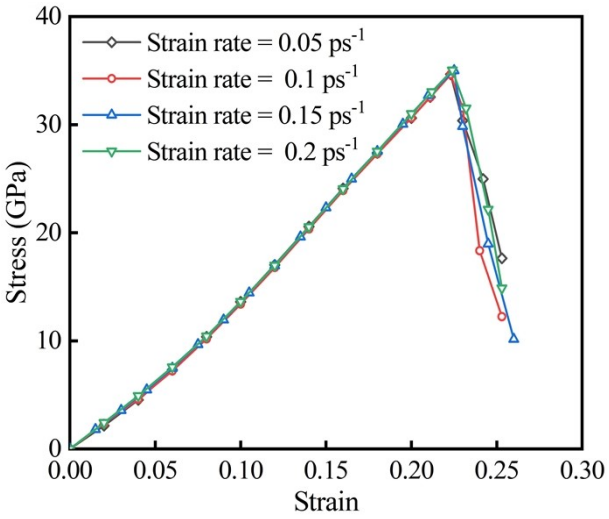

Fig. S1. Stress-strain relationship of boron carbide at different shear strain rates

It can be seen from Figure S1 that the shear stress-strain curves of boron carbide at different strain rates are almost consistent. Therefore, the loading strain rate has little influence on the research in this paper. It indicates that it is reliable to use loading strain rate of 0.1 ps^{-1} to calculate the shear stress-strain relationship in the MD calculations of this study.

Supplementary Note 3: The details of the twin model and classical MD simulations

The models chosen for the MD simulation of the shear tests are rectangular shape obtained from the original boron carbide rhombohedral unit cell by orthogonal transformation. Then, we performed shear simulations along the $(01\bar{1}\bar{1})/<\bar{1}101>$ slip system. For calculation convenience we rotated the shear model so that the x-z plane is the slip plane and the x direction is the slip direction in the Cartesian coordinate system. Finally, we obtained the dimensions of the boron carbide supercell in the x, y, and z directions are 28.48nm, 4.157nm, and 21.81nm, respectively. The total number of atoms is 345 600.

For the single-crystal and twinned structures, we first optimized the atomic positions and cell parameters to minimize the potential energy and geometries using the conjugate

gradient algorithm. The minimization process was stopped after the change in the total potential energy between two consecutive time steps reaches 1.0×10^{-10} eV. Then, we carried out isothermal-isobaric (NPT) ensemble to relax the model at 1 K using the Nosé-Hoover thermostat and barostat (50-fs damping constant for temperature and 2000-fs damping constant for pressure). The model was relaxed for 50 ps under the NPT ensemble, and the residual stresses after relaxing were less than 0.5 GPa. The temperature control under the NVT ensemble was implemented using the "fix nvt/sllod" module of LAMMPS, and the shearing process was implemented using the "fix deform" module of LAMMPS. The integration time step was set to 0.25 fs.

Supplementary Note 4: Thermal stability of nanotwinned boron carbide

For twinned boron carbide, its low density, extreme hardness, and high wear resistance make it an excellent candidate for lightweight bulletproof armor. However, the thermal stability of twinned boron carbide also directly affects its feasibility in armor applications. Here we employ molecular dynamics simulations to study the thermal stability of twinned boron carbide (taking the eight-layer twinned structure as an example). We performed extensive relaxation calculations for twinned boron carbide below 1200 K with precision of 10 K. Each temperature point was run for 50,000 steps with a time step of 0.25 fs under the NPT ensemble. As the relaxation temperature increases, we find that the thermal fluctuations inside the twinned boron carbide become more and more intense. The simulation results show that twinned boron carbide is stable below or equal to 1020 K. When the temperature reaches 1030 K or above, the crystal structure of twinned boron carbide is gradually deconstructed under the action of thermal fluctuations, as shown in Fig. S2(a)~Fig. S2(d). At

this time, the icosahedral structure collapses at high temperature and cannot maintain the original cage structure. Subsequently, the three-atom chain structure begins to bend, eventually leading to local amorphization of twinned boron carbide. This result obtained by classical MD shows that twinned boron carbide still maintains thermal stability up to 1020 K, which undoubtedly broadens the prospects for the manufacture and application of twinned boron carbide in the field of lightweight bulletproof armor.

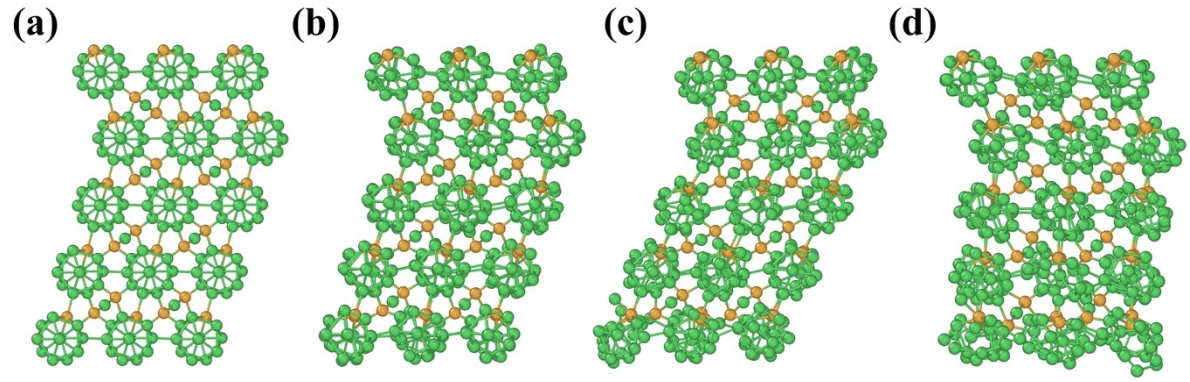

Fig. S2. Structural snapshots of twinned boron carbide producing amorphization at 1030 K. (a) step 0. (b) step 5000. (c) step 12000. (d) step 15000.

References

1. An, Q.; Goddard III, W. A., Atomistic origin of brittle failure of boron carbide from large-scale reactive dynamics simulations: Suggestions toward improved ductility. *Physical review letters* **2015,** *115* (10), 105501.
2. Ivashchenko, V.; Shevchenko, V.; Turchi, P., First-principles study of the atomic and electronic structures of crystalline and amorphous B 4 C. *Physical Review B* **2009,** *80* (23), 235208.
3. Li, X.; Liu, L.; Mei, H.; Xu, S.; Li, J.; Zhang, J., The formation mechanisms of amorphous bands of boron carbide nanopillars under uniaxial compressions and their effects on mechanical properties from molecular dynamics simulation. *Computational Materials Science* **2021,** *199*, 110708.
4. Morosin, B.; Kwei, G.; Lawson, A.; Aselage, T.; Emin, D., Neutron powder diffraction refinement of boron carbides nature of intericosahedral chains. *Journal of alloys and compounds* **1995,** *226* (1-2), 121-125.
5. Beaudet, T. D.; Smith, J. R.; Adams, J. W., Surface energy and relaxation in boron carbide (1011) from first principles. *Solid State Communications* **2015,** *219*, 43-47.
6. Bylander, D.; Kleinman, L.; Lee, S., Self-consistent calculations of the energy bands and bonding properties of B 12 C 3. *Physical Review B* **1990,** *42* (2), 1394.
7. Awasthi, A. P.; Subhash, G., High-pressure deformation and amorphization in boron carbide. *Journal of Applied Physics* **2019,** *125* (21), 215901.
8. DeVries, M.; Subhash, G.; Awasthi, A., Shocked ceramics melt: An atomistic analysis of thermodynamic behavior of boron carbide. *Physical Review B* **2020,** *101* (14), 144107.
9. Li, X.; Yang, X.; Mei, H.; Liu, L.; Xu, S.; Zhang, J., Boron carbide nanopillars under impact loading: Mechanical response and amorphous bands formation mechanism. *Computational Materials Science* **2022,** *214*, 111746.
10. Cheenady, A. A.; Awasthi, A.; DeVries, M.; Haines, C.; Subhash, G., Shock response of single-crystal boron carbide along orientations with the highest and lowest elastic moduli. *Physical Review B* **2021,** *104* (18), 184110.
11. Çekil, H. C.; Özdemir, M., The behaviour of Boron Carbide under shock compression conditions: MD simulation results. *Computational Materials Science* **2022,** *201*, 110872.
12. Bystrenko, O.; Jiang, J.; Dong, F.; Li, X.; Qiu, J.; Liu, J.; Zhang, J., Kinetics of bonds at structural breakdown in boron carbide under intensive loads: A molecular dynamics study. *Computational Materials Science* **2020,** *180*, 109711.